Oxygen Diffusion in Copolymers of Ethylene and Norbornene

Lars Poulsen,[†] Ingo Zebger,[†] Markus Klinger,[†] Morten Eldrup,[‡] Peter Sommer-Larsen,[‡] and Peter R. Ogilby*[,†]

Department of Chemistry, University of Aarhus, Langelandsgade 140, DK-8000 Århus, Denmark, and Risø National Laboratory, DK-4000 Roskilde, Denmark

Received June 3, 2003; Revised Manuscript Received July 22, 2003

ABSTRACT: Oxygen diffusion coefficients, *D*, have been measured as a function of temperature over the range 5−35 °C in films of poly(ethylene-*co*-norbornene). In the technique employed, the time evolution of oxygen sorption into the film was monitored using the phosphorescence of singlet oxygen as a spectroscopic probe. Many properties of these amorphous glassy materials depend significantly on the ethylene-to-norbornene ratio in the copolymer. For example, for samples in which the norbornene content in the copolymer was increased from 35 to 62%, the glass transition temperature of the material increased over the range 79−178 °C. Nevertheless, with these same changes in chemical composition, values of D(25 °C) varied only slightly over the range (2−6) × 10^{-8} cm^2 s^{-1}, and values of the apparent diffusion activation energy, E_{act}, varied slightly over the range 35−40 kJ mol^{-1}. The values of D(25 °C) obtained correlate reasonably well with calculated values of the polymer free volume as well as with the average free volume cavity size determined for these samples using positron annihilation lifetime spectroscopy. These data are consistent with models of diffusion that are based on the dynamic redistribution of local voids of critical volume into which the diffusing molecule can move. This study thus provides the foundation for attempts to regulate oxygen transport in these technologically and industrially important materials.

Introduction

Quantifying, understanding, and ultimately controlling the diffusion of small molecules in amorphous glasses are critical to the development and use of many polymeric materials.[1−4] The diffusion of molecular oxygen is particularly important. On one hand, as a diatomic molecule, oxygen is a representative small molecule that can be used to probe a range of general phenomena related to the interaction(s) between the penetrant and the host matrix. On the other hand, oxygen has many unique properties that distinguish it from other small molecules.[5] In particular, oxygen is a key participant in many processes that result in polymer degradation and in the degradation of materials that a given polymer may be designed to protect.[6,7] Embodied in this latter point is the importance associated with the development of polymeric oxygen barrier materials. Of course, given the earth's atmosphere and materials in equilibrium with the earth's atmosphere, oxygen is ubiquitous.

Approximately 10 years ago, we developed a spectroscopic technique to quantify oxygen diffusion coefficients in polymer films.[8] We have since used this tool to address a variety of issues related to the diffusion of oxygen in glassy polymers.[9−11] In this approach, oxygen sorption into the polymer is monitored using the near-infrared phosphorescence of singlet oxygen, $O_2(a^1\Delta_g)$, as the spectroscopic probe [$O_2(a^1\Delta_g) \rightarrow O_2(X^3\Sigma_g^-) + h\nu$ (∼1270 nm)]. In our studies thus far, singlet oxygen has been produced by energy transfer to ground-state oxygen, $O_2(X^3\Sigma_g^-)$, from a photosensitizer dissolved in the polymer. Upon exposure of a degassed polymer sample to an ambient atmosphere containing oxygen, the time-dependent singlet oxygen signal thus observed reflects the rate of oxygen sorption by the sample. In turn, for a sample of known thickness, l, these data directly yield the oxygen diffusion coefficient, D. For diffusion coefficients recorded as a function of temperature, an apparent activation energy, E_{act}, for the events associated with this diffusion can be obtained from Arrhenius plots of the data.

Over the past decade, the development of metallocene-catalyzed polymerization reactions has made it possible to prepare a host of new materials.[12] Of particular interest have been polymeric saturated hydrocarbons derived from the random copolymerization of ethylene or propylene, for example, with bulky cycloolefins.[12,13] Unlike the homopolymers poly(ethylene) and poly(propylene), which are semicrystalline, the cycloolefin copolymers are generally amorphous. The latter is simply a consequence of the cycloolefin "disrupting" the packing of homopolymeric segments. In turn, materials that have a range of unique properties can be prepared simply by altering the relative amount of cycloolefin used in the copolymerization.[12]

Scheme 1

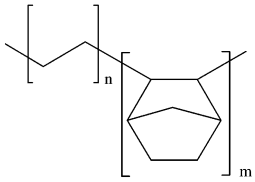

One series of commercially available cycloolefin copolymers is derived from the polymerization of ethylene and norbornene (Scheme 1).[12] These particular copolymers are transparent in the visible and UV regions of the spectrum, have a low birefringence, and do not fluoresce. As a consequence, they are ideal candidates for use as optical components, including lenses and compact disks.[14] Moreover, these copolymers are good electrical insulators and excellent water barriers and

[†] University of Aarhus.
[‡] Risø National Laboratory.
* To whom correspondence should be addressed: e-mail progilby@chem.au.dk.

10.1021/ma034744j CCC: $25.00
Published on Web 08/23/2003

Table 1. Properties of the Poly(ethylene-*co*-norbornene), EcN, Samples Used in This Study

	EcN(35) [TOPAS 8007]	EcN(51) [TOPAS 6013]	EcN(57) [TOPAS 6015]	EcN(62) [TOPAS 6017]
norbornene content (mol %)	35	51	57	62
T_g (°C)	78.8	139.9	159.9	177.8
M_n (g mol^{-1})	34000	50000	46000	49000
M_w (g mol^{-1})	116000	102000	125000	135000
polydispersity index	3.4	2.0	2.7	2.7
density (g cm^{-3})	1.002 ± 0.001	1.015 ± 0.001	1.019 ± 0.001	1.023 ± 0.001

can have glass transition temperatures, T_g, well in excess of 100 °C. Thus, these materials are also useful in the manufacture of devices and/or packaging,[14] particularly for the medical industry where sterilization by heating is commonly employed.

It is possible to significantly alter properties of these ethylene−norbornene copolymers, such as the glass transition temperature, simply by changing the ethylene/norbornene ratio in the copolymer.[12] With this in mind, we set out to investigate how such changes in the chemical composition of the copolymer influence both the oxygen diffusion coefficient, D, and the apparent diffusion activation barrier, E_{act}, obtained from experiments performed as a function of temperature. On a more general level, very few studies have, to our knowledge, systematically examined the influence of copolymer chemical composition on gas diffusion.[15,16]

Experimental Section

The instrumentation and approach used to spectroscopically monitor the time evolution of oxygen sorption into polymer films have been described.[8−11] The positron annihilation lifetime measurements were performed using an approach and instrumentation that have likewise been described.[17] Permeability measurements were performed using the "oxtran" instrument manufactured by MOCON, Inc.

The four cycloolefin copolymers used in this study were obtained from Hoechst Ticona, Germany. The material was received in the form of pellets and was used without further purification. In the nomenclature of Hoechst Ticona, the materials used were TOPAS 8007, 6013, 6015, and 6017, respectively. The acronym TOPAS derives from the phrase thermoplastic olefin polymer of amorphous structure. To better facilitate our discussion, however, we refer to these copolymers of ethylene and norbornene with the acronym EcN. When it is desirable to identify a material with a specific norbornene content, the mol % of norbornene is added in parentheses. Thus, a sample of poly(ethylene-*co*-norbornene) that consists of 35% norbornene is denoted EcN(35).

The oxygen sorption experiments were performed using tetrakis(4-tetradecyloxymethylphenyl)porphine, so-called lipo-TPP (Porphyrin Systems, Germany), as the singlet oxygen photosensitizer. In samples that contain dissolved oxygen, singlet oxygen is efficiently produced upon irradiation of lipo-TPP at 420 nm. When preparing the polymer samples, the amount of sensitizer used was adjusted to yield an absorbance at 420 nm of ∼0.3−0.6 in the final film. This corresponds to a sensitizer concentration of $\sim(1-2) \times 10^{-3}$ M in the film. At such concentrations, the presence of the sensitizer does not perturb oxygen diffusion in the polymer.[8,9]

EcN films used in the oxygen sorption experiments were prepared by spin-casting using a Headway Research model EC101DT-R790 photoresist spinner. In a typical procedure, the EcN pellets and the singlet oxygen sensitizer were dissolved in benzene. The amount of polymer used was generally 10−20 wt %. The benzene solutions of polymer and sensitizer were maintained at 60 °C for 2 h to achieve homogeneity and then were spin-cast onto glass plates that were likewise maintained at ∼60 °C. A typical spinning speed was between 3000 and 7000 rpm. After standing for 24 h at ambient temperature and pressure, the spin-cast films were then placed under vacuum for 24 h. Finally, the films were annealed at 50 °C for 24 h under vacuum using a Lab-Line Duo-Vac oven (model 3620-ST-1). Under these conditions, films with a thickness in the range ∼8−16 μm were generally produced.

It is important to note at this juncture that, under these preparative conditions, the behavior of EcN(62) was slightly different than that of the other three copolymers of ethylene and norbornene. Specifically, EcN(62) did not dissolve particularly well in benzene, and even after heating, the solution did not appear fully homogeneous. Rather, solutions of the polymer appeared to have two "phases" of different viscosity, and good quality films could be cast only from the less viscous material. On the other hand, when examining other properties of these copolymers (Table 1), we were unable to observe anything particularly unusual about the EcN(62) material used other than a weight-average molecular weight that is perhaps slightly larger than that for the other copolymers. In this same vein, it is likewise important to note that we had similar difficulties in dissolving the other EcN copolymers after they had been stored for over 2 years at ambient temperature.

In this study, the film thickness is an important parameter. Thus, to enhance the accuracy of our data, three independent methods were used to quantify film thicknesses. In the first, a microscope attached to a Fourier transform IR spectrometer was used to record interference fringes in the reflection−absorption spectrum of the polymer (i.e., the sample was placed on a reflective gold mirror). A Bruker IRscopeII connected to a Bruker IFS-66v/S spectrometer was used for this work. In this approach, the sample thickness, l, is obtained from the period of the interference fringes, $\Delta\nu$, via the relation $l = (2n\Delta\nu)^{-1}$, where n is the refractive index of the polymer.[18,19] In a given spectrum, the interference fringes were evaluated over the range ∼1500−2300 cm^{-1}. In the second method, the film thickness was determined via the Lambert−Beer relation using the UV/vis absorbance of the photosensitizer dissolved in the film. In the third method, a profilometer (DEKTAK V200SI) was used to quantify the film thickness. For a given film, the thicknesses obtained via these independent techniques were consistent with each other.

The positron annihilation lifetime experiments were performed with spin-cast EcN films as well as with thicker EcN plates. EcN films were prepared in the same way as described above with the exception that the sensitizer was not incorporated into the polymer. The annealed films were peeled-off of the glass plate, cut into small rectangles (∼8 × 12.5 mm), and stacked to yield a total sample thickness of ∼0.8 mm (i.e., a stack of ∼80 layers). EcN plates were prepared by heat-pressing the polymer pellets at 100 °C above the respective values of T_g using a press (F.S. Carver, Inc., model C) that was equipped with a film-pressing tool (Specac Inc.). The latter consisted of heated platens, two polished stainless steel pressing plates, disposable aluminum wafers between which the polymer pellets were placed, and calibrated spacers to control the thickness of the films. In a typical preparation, the polymer pellets were first heated to the desired temperature, held at this temperature for about 6 min to render the polymer melt homogeneous, and then pressed for 1 min at 1.5 tons. Upon releasing the pressure, the steel plates containing the sample were cooled to room temperature using a water-cooled heat sink (Specac Inc.). The polymer film was then removed from the pressing plates, and the aluminum wafers peeled away. Plates 100 μm thick were prepared and then stacked to yield a total sample thickness of 1 mm.

EcN samples used for the permeability experiments were likewise prepared by heat-pressing. The thickness of the samples used was typically 100 μm.

The glass transition temperatures of the EcN samples were determined using differential scanning calorimetry performed at a rate of 10 °C min^{-1} (PL-Thermal Sciences). The densities of the EcN samples were determined using a Mettler AE-100 analytical balance equipped with a model ME-33360 density determination kit. For these measurements, the sample dimensions used were ~1 × 1 × 0.1 cm, and the reference liquid was 99.9% methanol.

Size exclusion chromatography (SEC) was used to characterize the molecular weights and molecular weight distributions of the EcN samples. The SEC system was composed of three columns: a 50 mm × 7.5 mm PLgel 5 μm guard, a 300 mm × 7.8 mm Waters Styragel HMW6E, and a 300 mm × 7.5 mm PLgel 5 μm mixed-D. A differential refractometer/viscometer (Viscotek model 200) and an optical detector for right angle scattered light (Viscotek model 600) were used to monitor the material eluted. The columns and the detectors were maintained at 20 °C. A mixture of 75 vol % tetrahydrofuran and 25% 1,3,5-trimethylbenzene was used as the eluent and was pumped through the system at a rate of 1.0 mL/min (Shimatzu LC-10AD HPLC pump). The light scattering and refractometer signals were calibrated to a 110 000 Da polystyrene standard that had a polydispersity of less than 1.01 (Waters part no. 41995).

Results and Discussion

1. Characterization of the EcN Samples. Four different copolymers of ethylene and norbornene were used in this study. Specific features of these respective samples of poly(ethylene-*co*-norbornene), EcN, are shown in Table 1.

As outlined in the Introduction, one of the principal variables of interest in this study is the ethylene/norbornene ratio in the copolymer. For the materials supplied by Hoechst Ticona, the norbornene content was assessed using ^{1}H NMR spectroscopy with the assignments of Bergström et al.[20] The data obtained indicated that the samples had a norbornene content that ranged from 35 to 62%. Although the norbornyl moiety in a given EcN sample can exist as one of three different stereoisomers (exo−exo, endo−endo, and exo−endo), the ^{13}C NMR spectra of our samples revealed no evidence of the endo−endo and exo−endo isomers. Furthermore, these same spectra were consistent with a random distribution of the ethylene and norbornene moieties. In this regard, as the norbornene content in a given sample increased, the percentage of norbornene−norbornene linkages in the polymer likewise increased. In the analysis of these data, the ^{13}C NMR assignments of Stothers et al. were used.[21]

The most pronounced effect of this change in the ratio of ethylene to norbornene moieties appears in the glass transition temperature, T_g, of the respective polymers. For the samples examined in this study, values of T_g ranged from 79 °C for EcN(35) to 178 °C for EcN(62). Moreover, the values of T_g obtained depend linearly on the norbornene content in the copolymer (Figure 1). This observation is consistent with that of Rische et al.[22]

2. Oxygen Diffusion Measurements. Upon the exposure of a degassed polymer film to an ambient atmosphere containing oxygen, the polymer sample sorbs oxygen until equilibrium is reached with the ambient atmosphere. This process of gas sorption can be monitored using the phosphorescence of singlet oxygen as a spectroscopic probe (Figure 2).

In the triplet state photosensitized production of singlet oxygen, such as that employed in the present study, the intensity of the singlet oxygen phosphorescence signal observed, I_Δ, is proportional to the fraction of sensitizer triplet states quenched by ground-state oxygen (eq 1).[8,11]

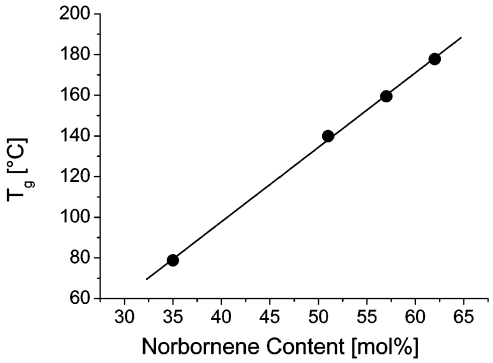

Figure 1. Plot of the glass transition temperature, T_g, for the four EcN samples studied against the norbornene content of the respective copolymer. The solid line is the result of a linear least-squares fit to the data. Errors on a given value of T_g are embodied in the size of the circle used to plot the data.

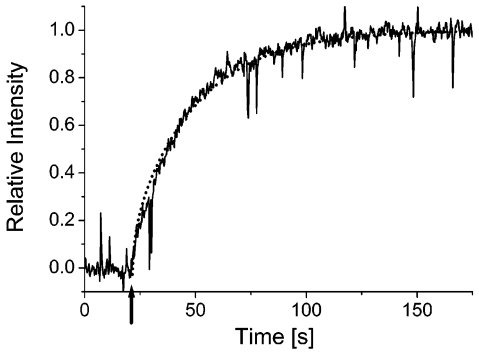

Figure 2. Singlet oxygen phosphorescence intensity recorded as oxygen is sorbed into a 10 μm thick film of EcN(51) cast onto a glass substrate. These data were recorded upon exposure of a degassed film to 40 Torr of oxygen (arrow indicates moment of exposure). The dotted line is the result of a fit of eq 2 to the data. The spikes on the trace reflect the response of our infrared detector to adventitious cosmic rays.

$$I_\Delta = \gamma \frac{k_q[O_2]}{k_q[O_2] + k_T} \qquad (1)$$

The proportionality constant γ includes a variety of parameters such as the efficiency of singlet oxygen radiative deactivation, the quantum efficiency of sensitizer triplet state formation, and instrumental parameters that account for signal collection efficiency and amplification.[8,11] In eq 1, k_q is the bimolecular rate constant for oxygen quenching of the sensitizer triplet state, and k_T is the sum of all rate constants for triplet state deactivation that are independent of oxygen. At low oxygen concentrations where $k_q[O_2] \ll k_T$, I_Δ depends linearly on the oxygen concentration in the polymer.[8,11] This can be seen in plots of the equilibrium singlet oxygen phosphorescence intensity, obtained from plots such as those shown in Figure 2, against the ambient oxygen pressure (Figure 3). Plots such as those shown in Figure 3 indicate that, for all the EcN samples examined, the intensity of the singlet oxygen phosphorescence signal observed is linearly proportional to the oxygen concentration in the sample under conditions in which the polymer is exposed to oxygen pressures less than 40 Torr. Thus, experiments to quantify oxygen

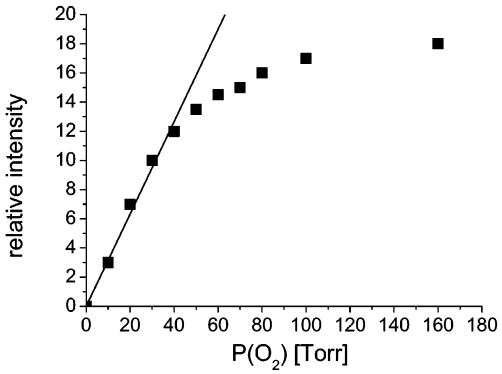

Figure 3. Plot of the equilibrium singlet oxygen phosphorescence intensity against the pressure of oxygen in the atmosphere surrounding the polymer sample. The equilibrium phosphorescence intensity is obtained from plots such as that shown in Figure 2 at times where the sample has reached equilibrium with the ambient atmosphere. These data were recorded from a sample of EcN(51) containing the sensitizer lipo-TPP. The solid line is the result of a linear least-squares fit to the data ≤ 40 Torr.

sorption into EcN films were performed by exposing degassed samples to an ambient atmosphere containing 40 Torr of oxygen.

Under conditions in which the intensity of the singlet oxygen phosphorescence signal is linearly proportional to the amount of oxygen that has been sorbed by the sample, data such as those shown in Figure 2 can be analyzed to yield the oxygen diffusion coefficient D. Specifically, using Fick's second law for one-dimensional diffusion, the time-dependent sorption plots behave according to the expression shown in eq 2.[8,11,23]

$$\frac{I_\Delta^t}{I_\Delta^\infty} = 1 - \sum_{n=0}^{\infty} \frac{8}{(2n+1)^2\pi^2} \exp\left(\frac{-D(2n+1)^2\pi^2 t}{4l^2}\right) \quad (2)$$

In eq 2, I_Δ^t and I_Δ^∞ represent the singlet oxygen phosphorescence intensity at times t and infinity, respectively, and l is the film thickness.

In iterative fits of eq 2 to data such as those shown in Figure 2, oxygen diffusion coefficients can be obtained under a variety of conditions. Of particular interest are diffusion coefficients obtained as a function of temperature, T. According to the Arrhenius relation (eq 3), plots of ln D against $1/T$ yield an apparent activation energy for diffusion, E_{act}.[9,10]

$$D = D_0 \exp\left(\frac{-E_{act}}{RT}\right) \quad (3)$$

Oxygen diffusion coefficients were obtained for the EcN samples over the temperature range 5−35 °C. Data obtained from the respective Arrhenius plots (e.g., Figure 4) as well as the diffusion coefficients recorded at 25 °C, D(25 °C), are listed in Table 2.

The data in Table 2 clearly indicate that, despite pronounced changes in some properties of the EcN samples as a function of the norbornene content (e.g., T_g), values of D(25 °C), E_{act}, and D_0 do not vary significantly with a change in the ethylene/norbornene ratio. Nevertheless, values of D(25 °C) appear to increase slightly with an increase in the norbornene content of the copolymer (Table 2, Figure 5). [At this juncture, when looking for apparent trends in the data, it is perhaps important to recall from the discussion in the Experimental Section that, when preparing the EcN films, EcN(62) did not behave in the same way as did the other copolymers.]

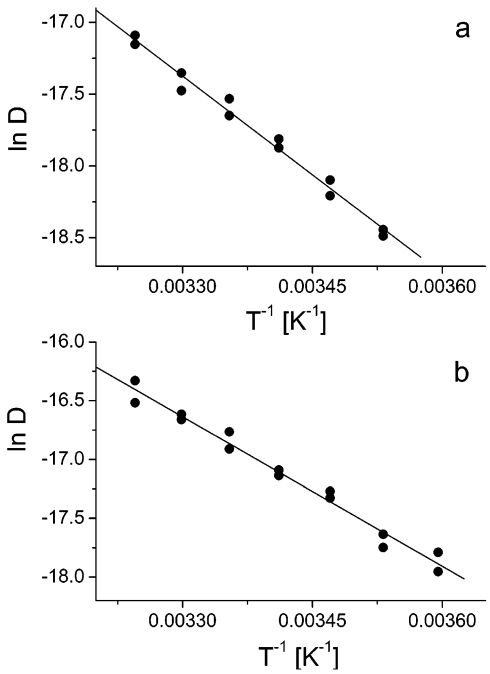

Figure 4. Arrhenius plots for the oxygen diffusion coefficient D in (a) EcN(35) and (b) EcN(62).

To our knowledge, oxygen diffusion coefficients have not previously been quantified in copolymers of ethylene and norbornene. On the other hand, values of D(25 °C) have been obtained from permeability (i.e., time lag) measurements on the homopolymers, poly(norbornene) and poly(ethylene). For poly(norbornene), Yampolskii et al.[24] report a value of D(25 °C) = 6.6×10^{-8} cm^2 s^{-1}. The latter is slightly larger than that observed in our experiments with EcN(57) and EcN(62) but, nevertheless, is consistent with our results given the apparent increase in D(25 °C) with an increase in the norbornene content. The diffusion coefficient of oxygen in poly(ethylene) is highly dependent on the degree of crystallinity in the given sample,[25] and values of D(25 °C) in the range $(1-5) \times 10^{-7}$ cm^2 s^{-1} have been reported.[26−28] Although these numbers are approximately 1 order of magnitude larger than those obtained in our experiments using the EcN sample with the smallest norbornene content (35%), this is not surprising since there are significant morphological differences between these materials. The values of D(25 °C) we obtained for the EcN samples, ranging from $\sim 2 \times 10^{-8}$ to 6×10^{-8} cm^2 s^{-1}, are similar to those observed in glassy poly(methyl methacrylate) and poly(carbonate) samples ($\sim(2-4) \times 10^{-8}$ and $\sim 6 \times 10^{-8}$ cm^2 s^{-1}, respectively).[9−11] The values of E_{act} obtained for the EcN samples, ranging from ∼35 to 40 kJ mol^{-1}, are likewise similar to those obtained, for example, from samples of glassy polystyrene ($E_{act} \sim 31$ kJ/mol) and polycarbonate ($E_{act} \sim 40$ kJ mol^{-1}).[9−11]

3. Oxygen Permeability Measurements. As mentioned in the previous section, the oxygen diffusion coefficient in many polymeric materials can also be quantified using a technique in which the oxygen flux through the polymer is measured as a function of time. In this approach, the so-called time-lag method,[1] the data yield the permeability, P, and the diffusion coef-

Table 2. Oxygen Diffusion Coefficients, D, Diffusion Activation Energies, E_{act}, and Arrhenius Preexponential Factors, D_0, for the Samples of Poly(ethylene-*co*-norbornene), EcN, Used in This Study

	EcN(35)	EcN(51)	EcN(57)	EcN(62)
D (25 °C) (cm^2 s^{-1})	$(2.2 \pm 0.3) \times 10^{-8}$	$(3.4 \pm 0.6) \times 10^{-8}$	$(5.8 \pm 0.8) \times 10^{-8}$	$(4.9 \pm 0.7) \times 10^{-8}$
E_{act} (kJ mol^{-1})	38.2 ± 1.5	39.6 ± 2.9	39.6 ± 2.0	35.2 ± 1.5
D_0 (cm^2 s^{-1})	0.11 ± 0.05	0.3 ± 0.2	0.5 ± 0.4	0.07 ± 0.04

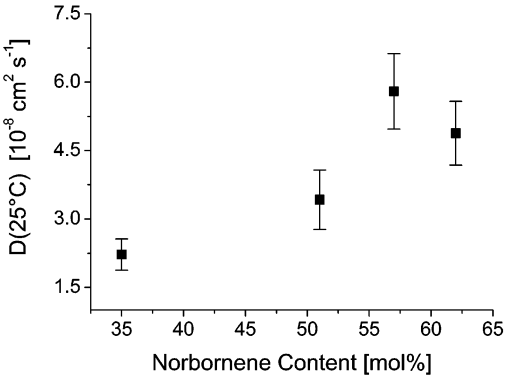

Figure 5. Plot of the oxygen diffusion coefficient recorded at 25 °C, D(25 °C), against the norbornene content for the four EcN samples examined.

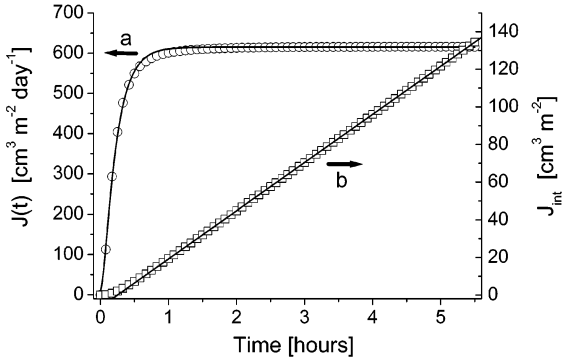

Figure 6. (a) Time dependence of the oxygen flux, $J(t)$, through a 100 μm thick sample of EcN(35). At time = 0, the sample was exposed to oxygen. Prior to this time, the sample was exposed to nitrogen for 17.5 h. The solid line reflects the fit of eq 4 to the data. (b) Plot of the integrated flux, J_{int} (i.e., the total amount of permeated oxygen), as a function of time for the same 100 μm thick sample of EcN(35). The permeability P was obtained from the slope of the line shown and the diffusion coefficient D from the intercept.

ficient, D. The solubility of oxygen in the given polymer, S, can then be estimated from the relation $S = P/D$.

With respect to quantifying the diffusion coefficient D, there are significant differences between the time-lag method and our sorption method. Each method has its advantages and disadvantages that, in turn, are reflected in the accuracy of the data recorded from a given sample. It is not the purpose of the present study, however, to address these differences. Rather, it is desirable to simply provide independent values of D(25 °C) for the EcN samples studied.

The oxygen flux, $J(t)$, through the EcN samples was monitored as a function of time (Figure 6a). The data obtained can be described using the appropriate solution to Fick's second law (eq 4),[1,29] where p is the oxygen pressure to which the sample is exposed and l is the film thickness. The permeability, P, and the diffusion coefficient, D, were obtained in iterative fits of eq 4 to the data (Table 3).

$$J(t) = \frac{Pp}{l}\left(1 + 2\sum_{n=1}^{\infty}(-1)^n \exp\left(-n^2\pi^2 \frac{D}{l^2} t\right)\right) \qquad (4)$$

Alternatively, using standard time-lag plots such as those shown in curve b in Figure 6, in which the integrated flux is plotted against time, values of the permeability, P, can be obtained from the slope of the data recorded under steady-state flux conditions, and values of D can be obtained from the intercept.

The accuracy of the data recorded in these permeability experiments is not particularly high. For example, note in Figure 6a that there is poor correspondence between the data and the model derived from eq 4. Nevertheless, within the error limits, the values of D(25 °C) obtained using the permeation approach agree with those obtained using our oxygen sorption method. Published values of the oxygen permeability in the homopolymer poly(norbornene) are in the range 2−10 barrers (1 barrer = 10^{-10} cm^3 (STP) cm s^{-1} cm^{-2} cmHg^{-1}).[24,30] Published values for the oxygen permeability in poly(ethylene) are somewhat smaller: 2−5 barrers for low-density poly(ethylene)[27,28] and 0.4 barrers for high-density poly(ethylene).[26] In comparison to these data on the homopolymers, the values of P obtained from the EcN samples appear reasonable.

Table 3. Oxygen Permeability, P, Diffusion Coefficient, D, and Solubility, S, Obtained from Time-Lag Oxygen Flux Experiments Performed at 25 °C

	EcN(35)	EcN(51)
P (barrer[a])	0.46 ± 0.05	0.73 ± 0.08
D (cm^2 s^{-1})	$(3.9 \pm 1.4) \times 10^{-8}$	$(2.7 \pm 0.6) \times 10^{-8}$
S (cm^3(STP) cm^{-3} atm^{-1})	$(9 \pm 3) \times 10^{-2}$	$(2.1 \pm 0.5) \times 10^{-1}$

[a] 1 barrer = 10^{-10} cm^3 (STP) cm s^{-1} cm^{-2} cmHg^{-1}.

4. Polymer Free Volume. The free volume of a polymer is defined as the difference between the total volume of a given sample, v, and the volume occupied by the polymer, v_0. The fractional free volume, FFV, is defined as

$$\mathrm{FFV} = \frac{v - v_0}{v} \qquad (5)$$

Because v and v_0 depend on the temperature of the given sample, it is expected that both the free volume and FFV will likewise vary with temperature.

In the free volume theory of diffusion, the motion of the penetrant depends on the dynamical redistribution of the free volume in the host medium.[31] Specifically, the diffusion of a molecule with a given volume through the host medium is governed by the probability of finding a void, or hole, in the host medium into which the penetrant can move. On this basis, Fujita[32,33] expressed the diffusion coefficient, D, for a given molecule using the following function

$$D = A_d \exp\left(-\frac{B_d}{\mathrm{FFV}}\right) \qquad (6)$$

where the parameters A_d and B_d reflect the size of the penetrant as well as interactions between the penetrant and host. Although the sample temperature, T, is not

Table 4. Values (in cm^3 mol^{-1}) of the Total Molar Volume, v, the van der Waals Volume, v_{vdw}, the Occupied Volume, v_0, and the Free Volume, $v - v_0$, for the Four Samples of poly(ethylene-*co*-norbornene), EcN, at 25 °C

	EcN(35)	EcN(51)	EcN(57)	EcN(62)
v^a	51.1	60.9	64.5	67.5
Van Krevelen[b]				
v_{vdw}	32.5	38.3	40.5	42.3
v_0[c]	42.3	49.8	52.7	55.0
$v - v_0$	8.8	11.1	11.8	12.5
Bicerano[d]				
v_{vdw}	34.9	41.5	44.0	46.1
v_0[c]	45.4	54.0	57.2	59.9
$v - v_0$	5.7	6.9	7.3	7.6

[a] The molecular weights of the monomeric units, ethylene and norbornene, were multiplied by the mole fraction of that monomeric unit in the polymer. The sum of these two terms was then divided by the density of the material. [b] Obtained using the Bondi/van Krevelen group contribution method.[36,37] [c] The occupied volume, v_0, is usually estimated as $v_0 = 1.3v_{vdw}$, where the factor of 1.3 accounts for packing densities at 0 K.[36] [d] Obtained using the Bicerano topology method.[38]

explicitly included in eq 6, it should be apparent from the expected functional dependence of FFV on T that the diffusion coefficient D, as expressed in eq 6, should likewise depend on temperature.

In the model from which eq 6 derives, it is assumed that diffusion is governed solely by the probability of finding a void of critical volume into which the penetrant can move. If an activation barrier, E_d, must be overcome in order for the penetrant to "jump" from one void to the next, eq 6 must be modified. To this end, the use of eq 7 has been proposed.[34,35]

$$D = A_d^{\ddagger} \exp\left(-\frac{E_d}{RT}\right) \exp\left(-\frac{B_d}{\mathrm{FFV}}\right) \qquad (7)$$

In eq 7, the term $\exp(-E_d/RT)$ defines the fraction of penetrant molecules that, at the temperature T, have sufficient energy to overcome the barrier E_d.

Given these principal tenets of the free volume theory of diffusion, we set out to ascertain whether norbornene-dependent differences in free volume could be a factor in establishing the magnitude of D(25 °C) in the EcN samples.

Calculated Free Volumes. The total molar volume v of a given material can be obtained from the molecular weight and density of the polymer. For this same material, the volume occupied by the polymer, v_0, depends on the van der Waals volume, v_{vdw}, of the macromolecule itself. Estimates of v_{vdw} can be obtained in several ways. In the van Krevelen/Bondi method, v_{vdw} is calculated as the sum of the van der Waals volumes of the individual functional groups that make up the macromolecule.[36,37] In the method of Bicerano,[38] the position of individual atoms in space (i.e., the topology of the system) is used along with the atomic van der Waals volumes to calculate v_{vdw}.

Using these respective methods, values of v_{vdw} were calculated for each of the EcN samples examined in this study (Table 4). To our knowledge, however, input parameters specific for the norbornyl system are not yet available for use with these methods (e.g., for the Bicerano approach, the topology of the system was created using the COMPASS force field[39] which lacks the appropriate norbornyl information). Thus, in performing these calculations, it was necessary to make some crude approximations, and not surprisingly, the values of v_{vdw} obtained using the van Krevelen approach differ from those obtained using the Bicerano approach. Nevertheless, the trends observed are the same. Specifically, the calculations indicate that the volume occupied by the polymer, v_0, increases with an increase in the norbornene content (Table 4). Although the total molar volume of the samples, v, likewise increases with an increase in the norbornene content, the increase in v is more pronounced. Thus, the amount of free volume in the samples, $v - v_0$, increases with an increase in the norbornene content. These points are illustrated in Figure 7.

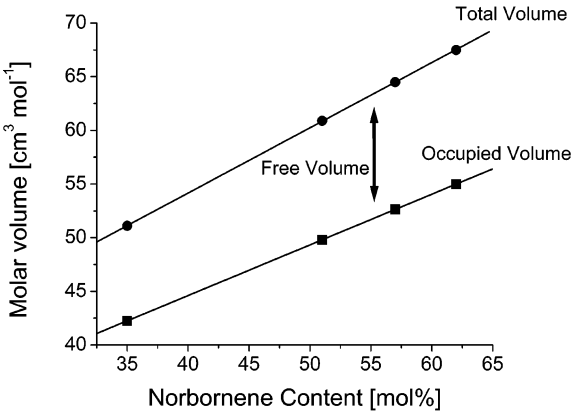

Figure 7. Plots of the total molar volume, v, and the volume occupied by the polymer, v_0, against the norbornene content in the four EcN samples. For the data shown, v_0 was calculated using the method of van Krevelen.[37] The solid lines are linear fits to the four data points. For a sample of a given norbornene content, the free volume, $v - v_0$, can be obtained as the difference between the lines shown (i.e., the double-headed arrow).

Unfortunately, the accuracy with which values of v_0 is obtained is sufficiently poor that, when taking the difference between v and v_0 (eq 5), the error in the resultant value of FFV is large enough to render any further analysis meaningless. Nevertheless, it indeed appears that, for the limited data set of EcN samples studied, D(25 °C) tends to increase with an increase in the free volume of the material. Specifically, the data appear to be consistent with what one might expect from models of diffusion that are based on free volume theory.

Positron Annihilation Lifetime Measurements. The correlation between experimental values of the oxygen diffusion coefficient, D(25 °C), and calculated values of the free volume provides some insight into the mechanism of oxygen movement in samples of glassy EcN. To further substantiate this perspective, however, it is desirable to experimentally ascertain whether the free volume in the EcN samples indeed changes in the way predicted by the van Krevelen and Bicerano calculations.

Positron annihilation lifetime spectroscopy (PALS) is a technique by which the free volume in polymers can be quantified.[17] A positron is an electron's antiparticle and, upon annihilation with an electron, emits radiation that can be detected in a time-resolved experiment.[40] Upon exposure of a polymer sample to a positron source, the decay of the positron population in the sample occurs via a number of processes, each of which occurs with a characteristic rate. Of particular interest to the problem at hand is a comparatively slow process that occurs over a period of several nanoseconds in which a metastable state of a positron and an associated electron, the so-called orthopositronium (o-Ps), decays by a

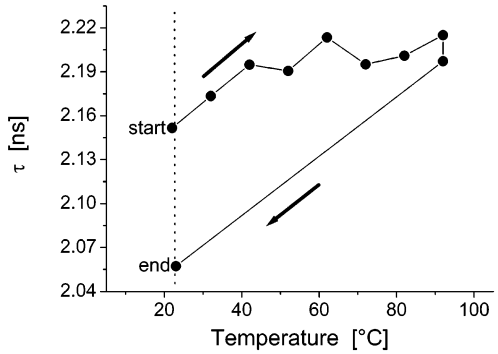

Figure 8. Plot of the orthopositronium lifetime, τ, obtained from PALS measurements against the temperature of the polymer sample. Data were recorded from a film of EcN(51) that had been solvent cast and then annealed in an oven at 50 °C (see Experimental Section). Exposure of this sample to temperatures as high as 90 °C in the PALS apparatus further annealed the sample. This is clearly evident in the heating-induced decrease in the value of τ recorded at 22 °C (dashed vertical line). The arrows show the direction in which the temperature of the sample was changed during this experiment.

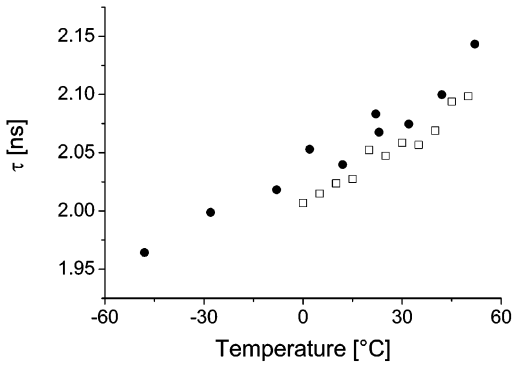

Figure 9. Plot of the orthopositronium lifetime, τ, obtained from PALS measurements against the temperature of the polymer sample. Data were recorded from samples of EcN-(51): (●) solvent cast film that had been heated to ∼90 °C in the PALS apparatus; (□) polymer plate that had been pressed at 240 °C.

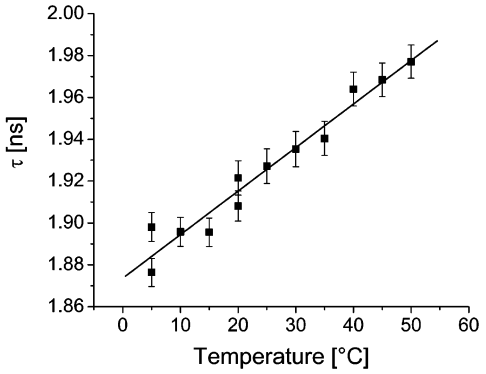

Figure 10. Plot of the orthopositronium lifetime, τ, obtained from PALS measurements against the temperature of the polymer sample. Data were recorded from EcN(35) plates that had been pressed at 180 °C. The solid line is a linear least-squares fit to the data.

mechanism that depends on the electron density of the surrounding environment. In short, the decay of this metastable state is slower in a material containing large voids than in a material containing smaller voids. Indeed, with the assumption of spherical voids, an estimate of the average void radius in the sample, R, can be obtained from the orthopositronium lifetime, τ-(o-Ps) (eq 8).[41,42] In turn, using the relation $V_f = 4\pi R^3/3$ for the average volume of a given void, an estimate of the free volume hole size in a sample can be obtained from PALS experiments.

$$\tau(\text{o-Ps}) = 0.5\left[1 - \frac{R}{R+\Delta R} + \frac{1}{2\pi}\sin\left(2\pi\frac{R}{R+\Delta R}\right)\right]^{-1} \quad (8)$$

In eq 8, ΔR is an empirical parameter equal to 1.66 Å and τ(o-Ps) is in ns.[41,42]

Data from PALS experiments were recorded from solvent-cast EcN films as well as from heat-pressed EcN plates. For each sample, values of τ(o-Ps) were obtained over a range of temperatures. In turn, values of V_f calculated using eq 8 could then be plotted as a function of temperature. At a given temperature, the slope of this latter plot defines the thermal expansion coefficient, α, of the cavities in the sample.

In performing the PALS experiments, it was immediately apparent that the temperature history of a given EcN sample is an important parameter that significantly influences the value of τ(o-Ps) recorded. This point is illustrated in Figure 8. In this experiment, τ(o-Ps) was obtained at 22 °C for a film of EcN(51) that had been solvent cast and then annealed in an oven at 50 °C (see Experimental Section). The temperature of the film was then increased in increments of 10 °C, and values of τ(o-Ps) were obtained at each stage of the proceedings. After having reached a temperature of 92 °C, which is still well below the T_g of 140 °C for this material, the sample was cooled and τ(o-Ps) was again recorded at 22 °C. The data indicate that this additional heating in the PALS chamber served to further anneal the sample which, in turn, reduced the average cavity volume by ∼9% at 22 °C (dashed vertical line in Figure 8). The effect of a sample's thermal history was also apparent in data recorded from EcN plates that had been heat-pressed at a temperature that was 100 °C higher than the T_g of the given material (Figure 9). Specifically, for a given EcN sample, values of τ(o-Ps) obtained from the heat-pressed plates were uniformly smaller than values of τ(o-Ps) obtained from a spin-cast film, even though that film had been "extra annealed" (i.e., heated to ∼90 °C in the PALS apparatus). The data shown in Figures 8 and 9 clearly indicate that, for the EcN samples examined in this study, annealing of solvent-cast films for 24 h at 50 °C is not sufficient to exclude further volume relaxation at temperatures above 50 °C. This point must thus be kept in mind as data from the respective experiments are compared. (See Appendix 1 for a related comment on how PALS data can be influenced by the solvent used for spin-casting the polymer film.)

PALS data were systematically recorded from plates of the EcN copolymers that had been pressed at 100 °C above the respective values of T_g. For these samples, orthopositronium lifetimes obtained over the range ∼0−50 °C varied linearly with the sample temperature (Figure 10). Using the linear regression from plots of τ(o-Ps) against T, we obtained an accurate value for τ-(o-Ps) at 25 °C as well as a value for $d\tau$(o-Ps)/dT. In turn, using eq 8, τ(o-Ps) was used to provide an estimate of the average cavity volume, V_f, in a given sample (Table 5).

The experimental data clearly indicate that values of τ(o-Ps) at 25 °C, and in turn V_f(25 °C), increase with an

Table 5. Lifetime of the Orthopositronium, τ(o-Ps), at 25 °C, Average Cavity Radius, R, Average Cavity Volume, V_f, and the Cavity Thermal Expansion Coefficient, α, for the Samples of Poly(ethylene-*co*-norbornene), EcN

	τ(o-Ps)[a] (ns)	R(25 °C)[b] (Å)	V_f(25 °C)[c] (Å^3)	α[d] (Å^3 °C^{-1})
EcN(35)	1.925 ± 0.003	2.786 ± 0.005	90.6 ± 0.2	0.19 ± 0.01
EcN(51)	2.047 ± 0.003	2.897 ± 0.005	101.9 ± 0.3	0.17 ± 0.02
EcN(57)	2.098 ± 0.003	2.945 ± 0.005	107.0 ± 0.3	0.16 ± 0.02
EcN(62)	2.158 ± 0.003	2.997 ± 0.005	112.7 ± 0.3	0.14 ± 0.02

[a] Obtained using the linear regression for data obtained over the range 0−50 °C. [b] Calculated from the orthopositronium lifetime using eq 8 with the assumption that the voids are spherical. [c] Obtained from the cavity radius R using the expression $V_f = 4\pi R^3/3$. [d] Obtained from plots of V_f against T.

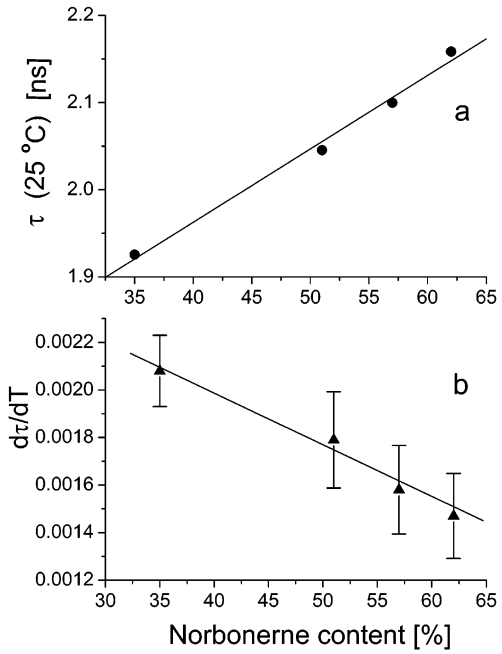

Figure 11. Plots of data obtained from PALS measurements against the norbornene content of the EcN copolymers. (a) Plot of the orthopositronium lifetime, τ, at 25 °C against the norbornene content. (b) Plot that shows the temperature dependence of the orthopositronium lifetime, dτ/dT, against the norbornene content. The solid lines are linear least-squares fits to the data.

increase in the norbornene content in the EcN copolymers (Figure 11a). Although methods have been proposed by which the fractional free volume, FFV, for a given material can be obtained from PALS data,[43] we rather defer to the work of Maurer and Schmidt[44] and simply say that the FFV is expected to depend linearly on values of V_f. Thus, we conclude that, in our EcN samples, FFV at 25 °C increases with an increase in the norbornene content.

The experimental data also clearly indicate that values of dτ(o-Ps)/dT and, hence, values of the thermal expansion coefficient of the free volume cavities, α, decrease with increasing norbornene content (Figure 11b).

5. The Mechanism of Diffusion. This study provides insight into the mechanism(s) by which oxygen transport is governed in these technologically and industrially important materials.

It is generally recognized that motions of polymer segments contribute significantly to the glass transition of a polymeric material.[45,46] The data on the present cycloolefin copolymers clearly indicate that changing the norbornene content in the copolymer has a pronounced effect on T_g. Thus, by association, it appears that one of the principal effects of this change in chemical composition is to alter features of the polymer that influence segmental motion in the macromolecule. On the other hand, the data indicate that despite these apparently significant changes in phenomena related to polymer segments, changes in both D(25 °C) and E_{act} are small. Thus, it appears that, for these copolymers, larger scale segmental motions of the macromolecule do not significantly influence oxygen diffusion. This conclusion is also consistent with the time scales involved for the respective processes (i.e., oxygen diffusion is a comparatively fast process, whereas segmental motion in polymer glasses is comparatively slow).

It is clear that the free volume in these polymer samples increases with an increase in the norbornene content (Table 5). Moreover, a reasonable correlation between values of D(25 °C) and the average cavity volume indicates that, in the samples studied, oxygen diffusion appears to be influenced by the probability of finding a local void of critical volume into which the penetrant can move. This is one of the fundamental tenets in the free volume theory of diffusion.

The data also indicate that there is an apparent activation barrier, E_{act}, for oxygen diffusion in these copolymers. Since this apparent barrier is essentially independent of changes in the norbornene content, it follows from the preceding discussion that this barrier likely derives from thermally dependent local phenomena, and not segmental phenomena, in the polymer. In short, oxygen diffusion is indeed determined by more spatially restricted phenomena in the polymer. This conclusion is consistent with observations made regarding oxygen diffusion in other polymer glasses.[9,10]

It is important to note that the PALS data recorded as a function of temperature yield thermal expansion coefficients for the free volume cavities that decrease with an increase in the norbornene content. From simple free volume considerations such as those embodied in eq 6, one might thus expect a corresponding change in the values of E_{act} (i.e., E_{act} would truly be an *apparent* barrier that derives solely from the way temperature-dependent changes in D reflect the cavity expansion coefficients α). The data, however, appear to indicate otherwise; within the errors of our experiment, values of E_{act} are essentially independent of changes in the norbornene content. This lack of correlation between α and E_{act} may indicate that the temperature dependence of D is due, in part, to processes other than the thermal expansion of the free volume cavities. For example, the temperature dependence of D could reflect thermally activated local motions of the polymer that, in turn, contribute to the dynamic redistribution of free volume in the sample and/or an activation barrier for the process in which oxygen "jumps" from one cavity to the next. In short, E_{act} would indeed reflect a *real* activation barrier. In this context, the present data thus indicate that changing the norbornene content in the copolymer does not have a significant effect on the thermally accessible local motions of the macromolecule.

Conclusions

Oxygen diffusion coefficients, D, and apparent diffusion activation barriers, E_{act}, have been measured in films of poly(ethylene-*co*-norbornene). For the samples used in this study, the norbornene content in the

copolymer ranged from 35 to 62%. This change in chemical composition is manifested in several ways. For example, the glass transition temperature of the material increases markedly as the norbornene content is increased and, for the samples studied herein, covers the range from 79 to 178 °C. Despite these rather pronounced differences, however, only slight changes were observed in both D(25 °C) and E_{act} as the norbornene content in the copolymer was varied over the same range. Nevertheless, the values of D(25 °C) obtained correlate reasonably well with calculated values of the polymer free volume and with the average free volume cavity size experimentally determined for these samples using positron annihilation lifetime spectroscopy. The data are consistent with models of diffusion that are based on the probability of finding a local void of critical volume into which the penetrant can move.

Acknowledgment. This work was supported by grants from the Materials Research Program of the Danish Research Council and from the Danish Polymer Center. The authors thank Ulf W. Gedde, Mikael Hedenqvist, and Janis Ritums for their hospitality and assistance with the oxygen permeation experiments performed at the Royal Institute of Technology in Stockholm, Sweden. This latter work was supported in a grant to Lars Poulsen through the European Science Foundation's SUPERNET program. The help of Mikkel Jørgensen, Walther Batsberg, Ole Hagemann, Lotte Nielsen, and P. S. Ramanujam, all of Risø National Laboratory, in the characterization of the polymer samples is gratefully acknowledged. Finally, we thank Dieter Ruchatz of Hoechst Ticona (Germany) for providing the samples of poly(ethylene-*co*-norbornene) used in this study.

Appendix 1

Effect of the Solvent used for Spin-Casting on the PALS Data. We have demonstrated that the thermal history of a given EcN sample influences the value of τ(o-Ps) obtained in the PALS experiment. In an independent series of experiments, we also discovered that the choice of solvent used for spin-casting the EcN films can likewise influence the results of the PALS experiment.

For EcN films cast from CCl_4, we discovered that the long-lived orthopositronium component was absent in the positron lifetime spectra. This is in contrast to data recorded from films cast from benzene, for which the orthopositronium component was clearly observed. It is known that CCl_4 is an efficient inhibitor of positronium formation.[47,48] Thus, the data appear to indicate that our samples contain amounts of residual CCl_4 sufficient to influence the PALS results. Indeed, upon rigorous heating of the samples that had been cast from CCl_4 to better facilitate removal of the residual solvent, the characteristic orthopositronium decay component could be observed in the positron lifetime spectra. For example, for a film of EcN(35) whose T_g is ~79 °C, it was necessary to keep the sample under vacuum at 150 °C for ~20 h before the intensity of the orthopositronium component was fully recovered. Upon cooling of this same sample, the expected temperature-dependent changes in τ(o-Ps) were observed, clearly revealing a transition that corresponds to T_g for this material (Figure 12).

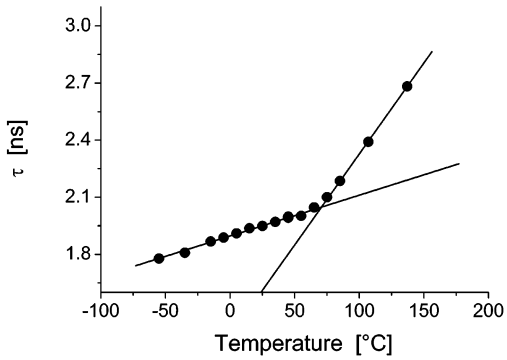

Figure 12. Plot of the orthopositronium lifetime, τ, obtained from PALS measurements against the temperature of the polymer sample. Data were recorded from films of EcN(35), cast from CCl_4, that had been kept under vacuum at 150 °C for ~20 h.

It should be noted that the PALS data in Figure 12 yield a T_g for EcN(35) that is ~8 °C less than that obtained from differential scanning calorimetry measurements (Table 1). This observation is entirely consistent with the rate at which the temperatures were changed in the respective experiments. Specifically, in the PALS experiment, the data at each temperature were acquired over a period of ~24 h. Thus, as the sample was cooled, the polymer had greater opportunity to make necessary conformational changes and thus could more closely approach equilibrium. On the other hand, the rate of temperature change in the differential scanning calorimetry experiments was 10 °C min^{-1}.

Appendix 2

Comment on Possible Surface Effects. It is reasonable to consider that the data recorded from comparatively thin samples could manifest, to a larger extent, phenomena associated with the surface of the film. Thus, for example, although the PALS data shown in Figure 9 could indeed be a consequence of the sample's thermal history, these same data could also reflect the more prominent effect of surface-related phenomena on the thinner samples. On the basis of the points outlined below, however, we conclude that, under all circumstances, our films are sufficiently thick and that the data always reflect phenomena associated with the bulk polymer; unique surface effects cannot be resolved.

For the PALS experiments performed under our conditions, surface effects on the o-Ps lifetime are limited to the outer ~25 nm in a given film.[49] Thus, for our experiments, in which the thinnest samples were ~8−16 μm thick, any surface-related effect will constitute only a small part of the overall signal recorded. With respect to the oxygen sorption experiments, we have repeatedly demonstrated in both the present and previous studies[8] that, for samples prepared under identical conditions, the diffusion coefficients obtained are independent of film thickness over the range ~10−100 μm.

In conclusion, although surface effects could, in principle, contribute to the phenomena monitored in our experiments, these effects are insignificant in our data. Rather, our data reflect phenomena associated with the bulk polymer.

References and Notes

(1) Vieth, W. R. *Diffusion In and Through Polymers*; Oxford University Press: New York, 1991.
(2) *Diffusion in Polymers*; Neogi, P., Ed.; Marcel Dekker: New York, 1996.
(3) *Polymeric Gas Separation Membranes*; Paul, D. R., Yampol'skii, Y. P., Eds.; CRC Press: Boca Raton, FL, 1994.
(4) *Barrier Polymers and Structures*; Koros, W. J., Ed.; ACS Symposium Series Vol. 423; American Chemical Society: Washington, DC, 1990.
(5) Sawyer, D. T. *Oxygen Chemistry*; Oxford University Press: New York, 1991.
(6) Schnabel, W. *Polymer Degradation*; Macmillan/Hanser: New York, 1981.
(7) Grassie, N.; Scott, G. *Polymer Degradation Stabilisation*; Cambridge University Press: Cambridge, 1985.
(8) Gao, Y.; Ogilby, P. R. *Macromolecules* **1992**, *25*, 4962−4966.
(9) Gao, Y.; Baca, A. M.; Wang, B.; Ogilby, P. R. *Macromolecules* **1994**, *27*, 7041−7048.
(10) Wang, B.; Ogilby, P. R. *Can. J. Chem.* **1995**, *73*, 1831−1840.
(11) Poulsen, L.; Ogilby, P. R. *J. Phys. Chem. A* **2000**, *104*, 2573−2580.
(12) Kaminsky, W. *Macromol. Chem. Phys.* **1996**, *197*, 3907−3945.
(13) Kaminsky, W.; Engehausen, R.; Kopf, J. *Angew. Chem., Int. Ed. Engl.* **1995**, *34*, 2273−2275.
(14) Cherdron, H.; Brekner, M.-J.; Osan, F. *Angew. Makromol. Chem.* **1994**, *223*, 121−133.
(15) Burns, R. L.; Koros, W. J. *Macromolecules* **2003**, *36*, 2374−2381.
(16) Raymond, P. C.; Koros, W. J.; Paul, D. R. *J. Membr. Sci.* **1993**, *77*, 49−57.
(17) Wang, C. L.; Hirade, T.; Maurer, F. H. J.; Eldrup, M.; Pedersen, N. J. *J. Chem. Phys.* **1998**, *108*, 4654−4661.
(18) Slayter, E. M.; Slayter, H. S. *Light and Electron Microscopy*; Cambridge University Press: Cambridge, 1992.
(19) Parkhutik, V.; Martinez, M. S.-J.; Senent, E. G. *J. Porous Mater.* **2000**, *7*, 239−242.
(20) Bergström, C. H.; Sperlich, B. R.; Ruotoistenmäki, J.; Seppälä, J. V. *J. Polym. Sci., Part A: Polym. Chem.* **1998**, *36*, 1633−1638.
(21) Stothers, J. B.; Tan, C. T.; Teo, K. C. *Can. J. Chem.* **1973**, *51*, 2893−2901.
(22) Rische, T.; Waddon, A. J.; Dickinson, L. C.; MacKnight, W. J. *Macromolecules* **1998**, *31*, 1871−1874.
(23) Crank, J. *The Mathematics of Diffusion*, 2nd ed.; Oxford Press: Oxford, 1975.
(24) Yampolskii, Y.; Shishatskii, S.; Alentiev, A.; Loza, K. *J. Membr. Sci.* **1998**, *149*, 203−220.
(25) Hedenqvist, M.; Gedde, U. W. *Prog. Polym. Sci.* **1996**, *21*, 299−333.
(26) Yasuda, H.; Stannett, V. In *Polymer Handbook*, 2nd ed.; Brandrup, J., Immergut, E. H., Eds.; Wiley: New York, 1975; pp III-229−III-240.
(27) Compañ, V.; López-Lidón, M.; Andrio, A.; Riande, E. *Macromolecules* **1998**, *31*, 6984−6990.
(28) Villaluenga, J. P. G.; Seoane, B. *J. Appl. Polym. Sci.* **2001**, *82*, 3013−3021.
(29) Sekelik, D. I.; Stepanov, E. V.; Nazarenko, S.; Schiraldi, D.; Hiltner, A.; Baer, E. *J. Polym. Sci., Part B: Polym. Phys.* **1999**, *37*, 847−857.
(30) Zhao, C.-T.; Ribeiro, M. d. R.; DePinho, M. N.; Subrahmanyam, V. S.; Gil, C. L.; DeLima, A. P. *Polymer* **2001**, *42*, 2455−2462.
(31) Cohen, M. H.; Turnbull, D. *J. Chem. Phys.* **1959**, *31*, 1164−1169.
(32) Fujita, H. In *Diffusion in Polymers*; Crank, J., Park, G. S., Eds.; Academic Press: London, 1968; p 75.
(33) Fujita, H.; Kishimoto, A.; Matsumoto, K. *Trans. Faraday Soc.* **1960**, *56*, 424−437.
(34) Vrentas, J. S.; Duda, J. L. *J. Polym. Sci., Polym. Phys. Ed.* **1977**, *15*, 403−416.
(35) Vrentas, J. S.; Duda, J. L. *J. Appl. Polym. Sci.* **1978**, *22*, 2325−2339.
(36) Bondi, A. *J. Phys. Chem.* **1964**, *68*, 441−451.
(37) VanKrevelen, D. W. *Properties of Polymers*, 3rd ed.; Elsevier: Amsterdam, 1990.
(38) Bicerano, J. *Prediction of Polymer Properties*, 2nd ed.; Marcel Dekker: New York, 1996.
(39) Sun, H. *J. Phys. Chem. B* **1998**, *102*, 7338−7364.
(40) Mogensen, O. E. *Positron Annihilation in Chemistry*; Springer-Verlag: Berlin, 1995.
(41) Tao, S. J. *J. Chem. Phys.* **1972**, *56*, 5499−5510.
(42) Eldrup, M.; Lightbody, D.; Sherwood, J. N. *Chem. Phys.* **1981**, *63*, 51−58.
(43) Yampolskii, Y. P.; Korikov, A. P.; Shantarovich, V. P.; Nagai, K.; Freeman, B. D.; Masuda, T.; Teraguchi, M.; Kwak, G. *Macromolecules* **2001**, *34*, 1788−1796.
(44) Maurer, F. H. J.; Schmidt, M. *Radiat. Phys. Chem.* **2000**, *58*, 509−512.
(45) *The Physics of Glassy Polymers*, 2nd ed.; Haward, R. N., Young, R. J., Eds.; Chapman and Hall: London, 1997.
(46) Gedde, U. W. *Polymer Physics*; Kluwer Academic Publishers: Dordrecht, 1995.
(47) Wikander, G.; Mogensen, O. E. *Chem. Phys.* **1982**, *72*, 407−423.
(48) Marques, M. F. F.; Burrows, H. D.; Miguel, M. d. G.; DeLima, A. P.; Gil, C. L.; Duplâtre, G. *Chem. Phys.* **1997**, *220*, 233−240.
(49) Cao, H.; Zhang, R.; Yuan, J.-P.; Huang, C.-M.; Jean, Y. C.; Suzuki, R.; Ohdaira, T.; Nielsen, B. *J. Phys.: Condens. Matter* **1998**, *10*, 10429−10442.

MA034744J